X-ray absorption near-edge spectra of overdoped $La_{2-x}Sr_xCuO_4$ high-T_c superconductors

Towfiq Ahmed,[1] Tanmoy Das,[2] J. J. Kas,[1] Hsin Lin,[2] B. Barbiellini,[2]
Fernando D. Vila,[1] R.S. Markiewicz,[2] A. Bansil,[2] and J. J. Rehr[1]

[1]*Department of Physics, University of Washington, Seattle, WA 98195*

[2]*Department of Physics, Northeastern University, Boston, MA 02115*

(Dated: January 31, 2011)

Abstract

We present results for realistic modeling of the x-ray absorption near edge structure (XANES) of the overdoped high-T_c superconductor $La_{2-x}Sr_xCuO_4$ in the hole doping range x = 0.20-0.30. Our computations are based on a real-space Green's function approach in which strong-correlation effects are taken into account in terms of a doping-dependent self-energy. The predicted O K-edge XANES is found to be in good accord with the corresponding experimental results in this overdoped regime. We find that the low energy spectra are dominated by the contribution of O-atoms in the cuprate planes, with little contribution from apical O-atoms.

I. INTRODUCTION

In their undoped parent compounds, high-T_c cuprate superconductors are antiferromagnetic insulators which are characterized by a gap driven by strong electron correlations. For this reason these materials are commonly referred to as Mott insulators. Strong correlation effects weaken with increased electron or hole doping, eventually yielding a metallic state. In $La_{2-x}Sr_xCuO_4$ (LSCO), for example, at a hole doping level of x $\sim$ 0.16, a paramagnetic state emerges and the material appears to recover Fermi liquid properties. However, despite over two decades of intense experimental and theoretical effort, the underlying principles governing how a Mott insulator transitions into a Fermi-liquid with doping are still not well understood.[1] The answer seems to be hidden within the mechanisms through which the quasiparticle spectral weight passes from the insulating Mott-Hubbard bands to the in-gap states near the Fermi level. In electron doped cuprates, the Mott gap and the associated lower Hubbard band can be directly probed by photoemission spectroscopy.[2,3] In the hole doped cuprates, on the other hand, this gap lies above the Fermi energy, so that techniques sensitive to empty states within a few eV above the Fermi energy must be deployed. Accordingly, light scattering techniques have been used, including optical, resonant inelastic x-ray scattering (RIXS), and x-ray absorption near edge spectroscopy (XANES) which probes the density of states (DOS) of empty states above the Fermi energy via excitations from core levels.[1,4–6]

The purpose of this study is to model the XANES spectrum of LSCO realistically, as an exemplar hole-doped cuprate, and to compare and contrast our theoretical predictions with available experimental data. The analysis is carried out using a real-space Green's function (RSGF) approach as implemented in the FEFF9 code.[7,8] Strong correlation effects on the electronic states near the Fermi energy (E_F) are incorporated by adding additional self-energy corrections to the one-particle electron and hole propagators. We concentrate in this initial study on the overdoped system because the cuprates are in a paramagnetic state in this doping range. Consequently the treatment of correlations effects is simpler, due to the absence of the pseudogap in the electronic spectrum. In LSCO, the pseudogap is found to vanish near x= 0.20.[1,3] We start with a generic plasmon-pole self-energy and then dress our calculations with a doping dependent paramagnetic self-energy Σ obtained within the self-consistent quasiparticle-GW (QP-GW) scheme.[1,9,10] Here GW refers to the Hedin

approximation to the self energy $\Sigma = iGW$, where G is the one-particle Green's function and W the screened Coulomb interaction.[11] This self-energy has been shown to capture key features of strong electronic correlations in various cuprate spectroscopies including ARPES[12], RIXS[13], optical[1] and neutron scattering[4], in good agreement with experiments in both electron and hole doped systems.

Many key properties of cuprates, including the physics of superconductivity, involve hybridized Cu $d_{x^2-y^2}$ and O $p_{x,y,z}$ orbitals near the Fermi energy E_F. Thus the natural choices for the probe atoms in which the incoming x-ray excites a core-hole are Cu and O. Since dipole selection rules do not allow K-edge excitations in Cu atoms to couple to d-bands, we focus here mainly on the O K-edge XANES. This edge may be expected to reflect doping dependent changes in the near E_F spectrum through its sensitivity to the O-p states. In O K-edge XANES experiments on LSCO,[14–16] two 'pre-peaks' have been observed to vary with Sr concentration. Our analysis indicates that the energy separation between these two peaks, which is comparable to the optical gap in the insulating phase,[1] is associated with the Mott gap.[17] In particular, the upper XANES peak corresponds to the empty states of the upper Hubbard band, and the lower peak to empty states in the lower Hubbard band resulting from hole doping. With increasing doping, the lower peak, which is absent for x = 0., starts to grow while the upper peak loses intensity. In the overdoped regime, the lower peak reaches a plateau,[18] while the intensity of the upper peak is substantially suppressed.

In order to assess effects of core-hole screening, we have also calculated the Cu K-edge XANES, again using the same RSGF approach.[7,8] In this connection, two different core-hole models were considered: (i) Full screening, i.e., without a core-hole as in the "initial state rule" (ISR),[19] and (ii) RPA screening as is typically used in Bethe-Salpeter equation (BSE) calculations.[20] Both of these core-hole models reasonably reproduce the experimental XANES of the O K-edge in the pre-peak region in overdoped LSCO.

The remainder of this article is organized as follows. Introductory remarks in Section I are followed by a brief account of the methodological details of the RSGF formalism in Section IIA, and of the QP-GW self-energy computations in Section IIB. XANES results based on the plasmon-pole self-energy are discussed in Section IIIA, while results based on doping dependent QP-GW self-energies are taken up in Section IIIB. Finally Section IV contains a summary and conclusions.

II. THEORY

A. Real-space Green's function formulation

Here we briefly outline the real-space Green's function multiple-scattering formalism underlying the FEFF code. More detailed accounts are given elsewhere.[7,8] The quasi-particle Green's function for the excited electron at energy E is defined as

$$G(E) = [E - H - \Sigma(E)]^{-1}. \tag{1}$$

Here H is the independent particle (i.e., Kohn-Sham) Hamiltonian,

$$H = \frac{p^2}{2} + V, \tag{2}$$

with V being the Hartree potential plus a ground state exchange-correlation density functional, which in FEFF9 is taken to be the von Barth-Hedin functional.[21] Throughout this paper Hartree atomic units ($e = \hbar = m = 1$) are implicit. This Hamiltonian together with the Fermi-energy E_F are calculated self-consistently using the RSGF approach outlined below. In Eq. (1) the quantity $\Sigma(E)$ is the energy-dependent one-electron self-energy. In this work we use a GW self-energy designed to incorporate the strong-coupling effects in cuprates, as discussed further in Section IIB below.

In the RSGF approach it is useful to decompose the total Green's function $G(E)$ as

$$G(E) = G^c(E) + G^{sc}(E), \tag{3}$$

where $G^c(E)$ is the contribution from the central atom where the x-ray is absorbed and $G^{sc}(E)$ is the scattering part. For points within a sphere surrounding the absorbing atom the angular dependence of the real space Green's function can be expanded in spherical harmonics as

$$G(\mathbf{r}, \mathbf{r}', E) = \sum_{L,L'} Y_L(\hat{\mathbf{r}})\, G_{L,L'}(r, r', E)\, Y^*_{L'}(\hat{\mathbf{r}'}). \tag{4}$$

Here, Y_L is a spherical harmonic and $L = (l, m)$ denotes both orbital and azimuthal quantum numbers. The physical quantity measured in XANES for x-ray photons of polarization $\hat{\epsilon}$ and energy $\omega = E - E_c$ is the x-ray absorption coefficient $\mu(\omega)$, where E_c is the core electron energy, and E is the energy of the excited electron. The absolute edge energy is given by $\omega = E_F - E_c$, where E_F is the Fermi level. The FEFF code calculates both $\mu(\omega)$, the site-

and l-projected DOS $\rho_l^{(n)}(E)$ at site n and the Fermi energy (E_F) self-consistently. These quantities can be expressed in terms of the Green's function in Eq. (4) as

$$\mu(\omega) \propto \; -\frac{2}{\pi}\mathrm{Im}\; \langle\phi_0|\hat{\epsilon}.\mathbf{r}G(\mathbf{r},\mathbf{r}',E)\hat{\epsilon}.\mathbf{r}'|\phi_0\rangle\,, \tag{5}$$

where $E = \omega + E_c$ and

$$\rho_l^{(n)}(E) = \; -\frac{2}{\pi}\mathrm{Im}\sum_m \int_0^{R_n} G_{L,L}(r,r,E)\, r^2\, dr\;, \tag{6}$$

respectively. Here $|\phi_0\rangle$ is the initial state of the absorbing atom and R_n is the Norman radius[22] around the nth atom, which is analogous to the Wigner-Seitz radius of neutral spheres, and the factor 2 accounts for spin degeneracy.

B. Self-energy corrections from strong correlations in cuprates

In the optimal or overdoped regime of present interest, cuprates do not exhibit any signature of a symmetry-breaking order parameter, and thus the quasiparticle dispersion can be well-described with a paramagnon-renormalized one band Hubbard model.[1] The details of the related self-energy are given in Ref. 9 and are summarized here for completeness.

In our QP-GW approach, we start with a tight-binding single band bare dispersion $\xi_{\mathbf{k}}$ where the parameters are obtained by fitting to the first-principles LDA dispersion.[23–25] The values of the tight-binding parameters used in LSCO are from Ref. 1. The LDA dispersion is then self-consistently dressed by the full spectrum of spin and charge fluctuations treated at the RPA level. The susceptibility can be written in terms of the bare susceptibility $\chi_0(\mathbf{q},\omega)$ as

$$\chi(\mathbf{q},\omega) = \frac{\chi_0(\mathbf{q},\omega)}{1-\bar{U}\chi_0(\mathbf{q},\omega)}. \tag{7}$$

Here $\bar{U}$ is the renormalized Hubbard U value. The imaginary part of the RPA susceptibility provides the dominant fluctuation interaction to the electronic system, which can be represented by $W(\mathbf{q},\omega) = (3/2)\bar{U}^2\chi''(\mathbf{q},\omega)$. The resulting self-energy correction to the LDA dispersion within the GW approximation is

$$\begin{aligned}\Sigma(\mathbf{k},\omega) \;&=\; Z\sum_{\mathbf{q}} W(\mathbf{q},\omega')\Gamma(\mathbf{k},\mathbf{q},\omega,\omega') \\ &\times\; \left[\frac{f(\bar{\xi}_{\mathbf{k}-\mathbf{q}})}{\omega+\omega'+i\delta-\bar{\xi}_{\mathbf{k}-\mathbf{q}}} + \frac{1-f(\bar{\xi}_{\mathbf{k}-\mathbf{q}})}{\omega-\omega'+i\delta-\bar{\xi}_{\mathbf{k}-\mathbf{q}}}\right],\end{aligned} \tag{8}$$

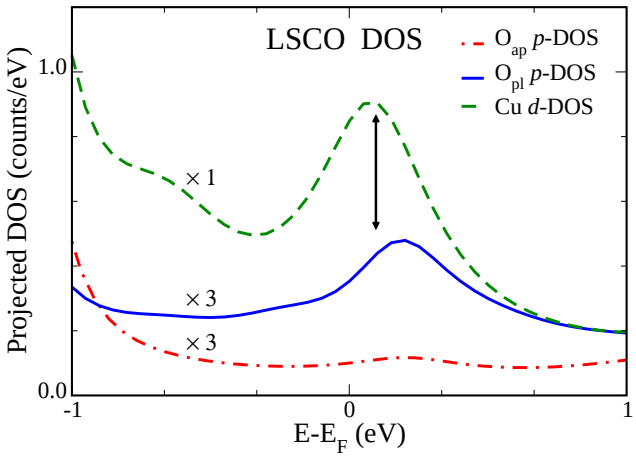

FIG. 1: (color online) Site- and l-projected DOS in doped LSCO, x= 0.30. Cu-d (green dashed line), O_{pl}-p (blue solid line) and O_{ap}-p (red dashed-dotted line) DOS are shown. Note scaling of the lower two curves by a factor of 3. Arrows mark the structure related to the van Hove singularity in the hybridized Cu-O bands discussed in the text.

where $f(\xi)$ is the Fermi function and Γ is the vertex correction defined below.

Different levels of self-consistency within the GW scheme involve different choices for χ_0 and dispersion $\bar{\xi}_{\mathbf{k}}$. Within our QP-GW scheme, the Green's function entering into the χ_0 bubble is renormalized by an approximate renormalization factor Z which is evaluated self-consistently. The corresponding vertex correction is taken within the Ward identity $\Gamma = 1/Z$, and $\bar{\xi}_{\mathbf{k}} = Z(\xi_{\mathbf{k}} - \mu)$ is the renormalized dispersion where μ is the chemical potential. The renormalized band is employed to calculate the full spectrum of spin susceptibility:

$$\chi_0(\mathbf{q},\omega) = -Z \sum_{\mathbf{k}} \frac{f(\bar{\xi}_{\mathbf{k}}) - f(\bar{\xi}_{\mathbf{k+q}})}{\omega + i\delta + \bar{\xi}_{\mathbf{k}} - \bar{\xi}_{\mathbf{k+q}}}. \tag{9}$$

The doping dependence of U is discussed in Refs. 1 and 4. A single, universal function $\bar{U}(x)$ is found to reasonably describe a number of different spectroscopies including photoemission, optical spectra[1] and the present XANES. This doping dependence is consistent with charge screening.[5]

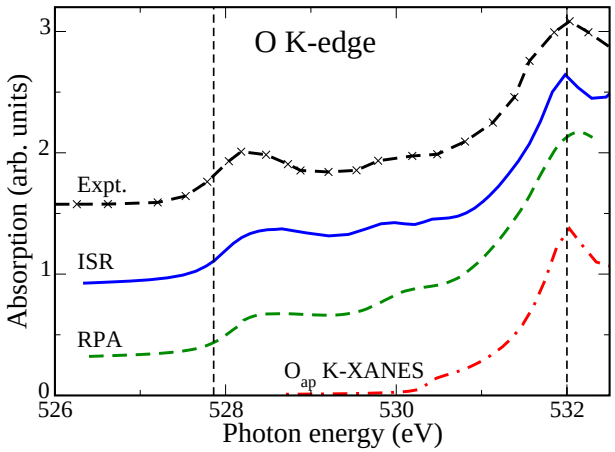

FIG. 2: (color online) Theoretical and experimental[26] O K-edge XANES spectra in overdoped LSCO (x=0.30). Computations where the core-hole is fully screened, i.e. using the initial state rule (ISR) (blue solid line) are compared with results based on RPA screened core-hole (green dashed line) and experiments (dashed crossed line). The vertical dashed line at 527.8 eV marks the edge energy $E_F - E_c$ which is sensitive to doping. A vertical dashed line is also drawn through the feature at 532 eV. This feature is due to the apical O, as shown by the red dashed-dotted line, calculated with the ISR.

III. RESULTS AND DISCUSSION

In Subsection IIIA below, we discuss O and Cu K-edge XANES using a generic GW plasmon-pole self-energy and RPA core-hole screening, but without the self-energy correction arising from strong correlation effects. Subsection IIIB examines doping-dependent effects of self-energy corrections on the O K-edge XANES.

A. XANES without self-energy corrections

Since K-edge XANES probes the site-dependent p-density of states (p-DOS), we consider first the projected p-DOS from O and Cu sites near E_F as obtained using the FEFF code. The low-temperature orthorhombic crystal structure with space group Bmab was used.[28] It is important to note that the structure involves two inequivalent O-atoms with different chemical environments, namely, the O-atoms in the cuprate planes (O_{pl}), and the apical

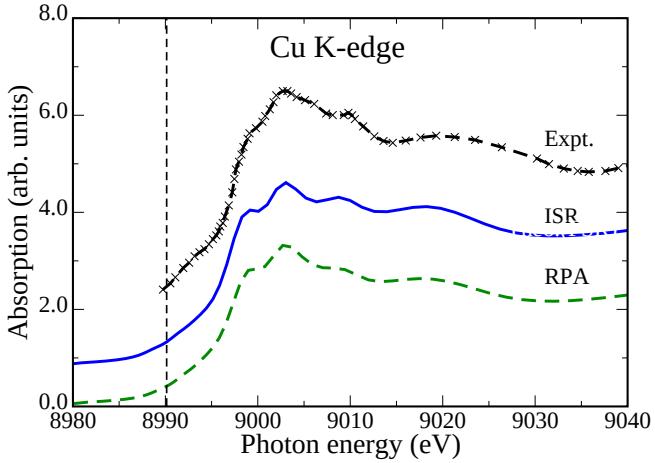

FIG. 3: (color online) Theoretical and experimental[27] Cu K-edge XANES spectra in undoped LSCO (x=0.). Curves have same meaning as in Fig. 2. The vertical dashed line at 8990 eV marks the edge energy $E_F - E_c$ as in Fig. 2.

O-atoms (O_{ap}) which lie in the La-O planes.[29,30] The projected densities of states on the two distinct O-atoms and the Cu-atoms are shown in Fig. 1. Also shown for reference is the projected d-DOS from Cu-sites, even though as already pointed out K-edge excitations do not couple with the d angular momentum channel. The p-DOS from the O-atoms in the cuprate planes (middle curve) is seen to display the structure marked by arrows, arising from the hybridization of localized Cu d and O p orbitals, which is related to the van Hove singularity (VHS) near E_F in the band structure of LSCO. The O_{ap} contribution is seen to be quite small and structureless within an energy range ± 0.75 eV of E_F, although a weak replica of the VHS peak suggests a small hybridization of the apical and in-plane oxygens. This implies that O K-edge XANES pre-peak is mainly associated with unoccupied electronic states from atoms lying in the Cu-O planes. Notably, the Cu-p DOS (not shown) in the near E_F energy window of Fig. 1 is also quite small and structureless and becomes significant only several eV above E_F. The experimental evidence for the aforementioned features of XANES spectra has been discussed previously by several authors.[14–16]

The treatment of core-hole screening in the O K-edge spectrum is addressed in Fig. 2, where we compare the experimental results from overdoped LSCO with computations using two different core-hole screening models. The computed XANES spectrum using a fully screened hole (blue solid curve) is seen to be in good accord with the results of the RPA

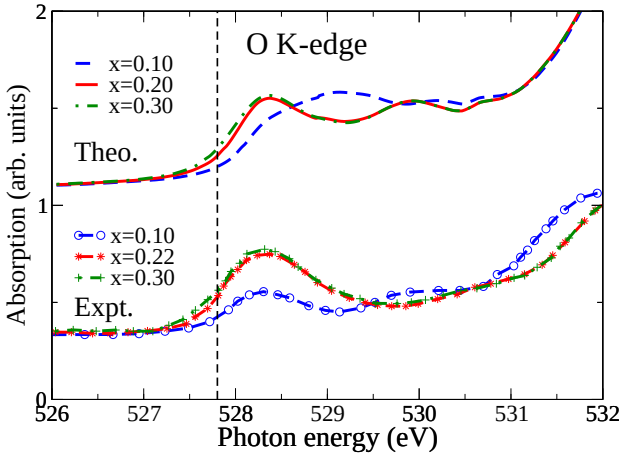

FIG. 4: (color online) Doping-dependent theoretical (upper curves) and experimental[18] (lower curves) O K-edge XANES spectra in LSCO. Computations include the effect of self-energy corrections of Eq. (8) resulting from strong correlation effects. Different dopings with different concentrations of x are shown by lines of various colors (see legend). The vertical line marks the edge energy $E_F - E_c$ as in Fig. 2.

screened hole (green dashed curve), although the intensity of the feature at 532 eV differs somewhat in the ISR and RPA results. All three curves in Fig. 2 show the presence of the pre-edge peak around 528.5 eV, a weaker pre-edge feature around 530 eV, and the prominent peak at 532 eV, which is due to the apical oxygen, as demonstrated by the calculated partial absorption, red (dashed-dotted) curve. Fig. 3 presents results along the preceding lines for the Cu K-edge XANES in undoped LSCO. Since the Cu K-edge probes p-states which are only weakly correlated, it provides a useful check of our theoretical method for the case of weak-correlation. The results in Figs. 2 and 3 clearly indicate that the K-edge spectra are not sensitive to the core-hole screening model, as both the RPA and the ISR give results in reasonable agreement with experiment.

B. Strong correlation effects and doping dependence

We emphasize that the conventional LDA-based formalism is fundamentally limited in its ability to describe the full doping dependence of the electronic structure of the cuprates, because the LDA yields a metallic instead of an insulating state in the undoped system.

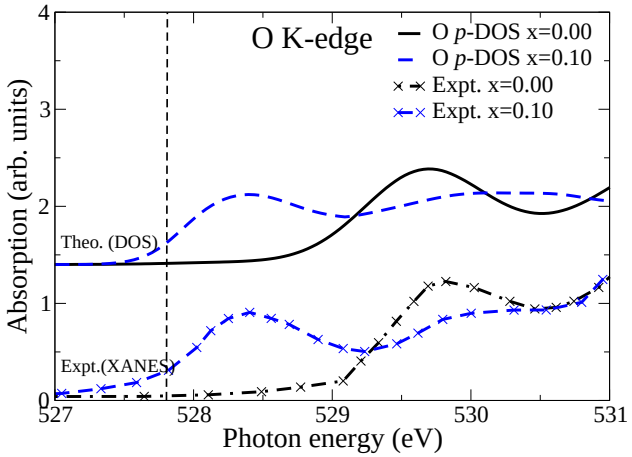

FIG. 5: (color online) O K-edge XANES from experiment[31] (lower set of broken curves) for x = 0. and x = 0.10, compared with theoretical single-band p-DOS (upper curves) for O_{pl} for x = 0. and x = 0.10.[4] The vertical line marks the edge energy $E_F - Ec$ as in Fig. 4.

Therefore, strong correlation effects must be added to properly model the doping evolution of electronic states. Fig. 4 compares recent experimental results[18] with the theoretical O K-edge XANES spectra in overdoped LSCO, where the self-energy correction Σ along the lines of Section IIB is included in the computations. Representative real and imaginary parts of Σ are shown in Ref. 1. Focusing first on the overdoped regime for hole doping concentration between x = 0.20 to x = 0.30, both theory and experiment display a small, systematic shift of the edge to lower energies with increasing doping. The low energy peak at 528.5 eV in Fig. 4 shows the experimental and theoretical edge regimes, showing that both display a similar shift of the Fermi level with doping. Otherwise, the XANES spectra undergo relatively little change in the overdoped system.

As the doping is further reduced, the intensity of the 528.5 eV peak decreases while a new peak appears near 530 eV and rapidly grows with underdoping until at x = 0., the 528.5 eV peak is completely gone. The remaining 530 eV peak represents the upper Hubbard band, and its shift in energy from the Fermi level is consistent with optical measurements.[1] Turning to the x = 0.10 spectra in Fig. 4, we see that, as expected, now theory differs substantially from experimental results. Although theory correctly reproduces the reduced intensity of the 528.5 eV peak, it does not show the observed enhanced intensity of the upper peak at 530 eV. Instead, the spectral weight is shifted halfway between the lower

and upper peaks. In Fig. 5, the experimental results indicate the opening of a gap in the spectrum which is not captured in our modeling. However, we were able to reproduce the experimental doping dependence[18] in a simpler calculation in which the XANES spectrum is modeled via the empty density-of-states, but in which self-energy corrections including the magnetic gap are incorporated.[4] Fig. 5 compares the experimental XANES spectrum with this DOS approximation at x = 0.10. The splitting of the spectrum into two peaks with the appropriate gap is well reproduced. It should be noted that this same self energy reproduced the optical and RIXS gaps as a function of doping.[1,5,13]

Interestingly, the good agreement between theory and experiment in the overdoped case implies that the upper peak at 530 eV possesses little weight in the overdoped system. In particular, we find a saturation of the lower energy feature (528eV) in the O K-edge spectra [Fig. 4] as the doping value is increased beyond the optimal doping, except for the Fermi edge shift. This saturation is in good agreement with the experiment by Peets et al.,[18] but is inconsistent with model calculations by Liebsch[32] and Wang et al.[33] This effect requires a transfer of spectral weight from the upper to the lower peak, which is much larger than that predicted by *t-J* models of the cuprates.[4] A similar conclusion was arrived at by Peets *et al.*[18] Such anomalous spectral weight transfer has been discussed in several spectroscopies of cuprates.[1,34,35] The present intermediate coupling calculations can provide a satisfactory explanation of these results.[3]

IV. SUMMARY AND CONCLUSIONS

We have carried out a realistic calculation of the XANES of the cuprate superconductor LSCO. Our focus in this first such attempt is on the O K-edge XANES in overdoped LSCO over the hole doping range x = 0.20 to x = 0.30. For this purpose, we have incorporated doping dependent self-energy corrections due to strong electron correlations into a real space Green's function formalism, which is implemented in the FEFF9 code. Good agreement is found between theoretical and experimental doping evolution of the XANES in overdoped LSCO. Although LSCO has two chemically distinct O-atoms, the O K-edge XANES is dominated by the contribution of O-atoms in the cuprate planes. Apical O-atoms only begin to make a significant contribution to the spectrum at higher energies greater than 531 eV. In examining effects of the core-hole screening, we find that the spectra are insensitive to

the core-hole screening model at least in the overdoped regime. In the underdoped case, as expected, our self-energy corrections, which are appropriate for the overdoped paramagnetic system, fail to correctly describe salient features of the spectra. A simple calculation suggests that correcting this will require a more comprehensive modeling of XANES including effects of pseudogap physics on the self-energies in the underdoped regime.

V. ACKNOWLEDGMENT

This work is supported by the Division of Materials Science & Engineering, Basic Energy Sciences, US Department of Energy Grants DE-FG03-97ER45623 and DE-FG02-07ER46352, and has benefited from the allocation of supercomputer time at NERSC and Northeastern University's Advanced Scientific Computation Center (ASCC). The research also benefited from the collaboration supported by the Computational Materials Science Network (CMSN) program of US DOE under grant DE-FG02-08ER46540.

[1] T. Das, R. S. Markiewicz, and A.Bansil, Phys. Rev. B **81**, 174504 (2010).

[2] C. Kusko, R.S. Markiewicz, M. Lindroos, and A. Bansil, Phys. Rev. B. **66**, 140513(R) (2002); A. Bansil, M. Lindroos, S. Sahrakorpi, and R.S. Markiewicz, New J. Phys. **7**, 140 (2005).

[3] R. S. Markiewicz, T. Das, and A. Bansil, Phys. Rev. B **82**, 224501 (2010).

[4] A.Bansil, S. Basak, T. Das, H. Lin, M. Lindroos, J. Nieminen, I. Suominen, and R. Markiewicz (2011), to be published.

[5] R. S. Markiewicz and A. Bansil, Phys. Rev. Lett. **96**, 107005 (2006).

[6] Y.W. Li, D. Qian, L. Wray, D. Hsieh, Y. Xia, Y. Kaga, T. Sasagawa, H. Takagi, R.S. Markiewicz, A. Bansil, H. Eisaki, S. Uchida, and M.Z. Hasan, Phys. Rev. B**78**, 073104 (2008).

[7] J. J. Rehr, J. J. Kas, F. D. Vila, M. P. Prange, and K. Jorissen, pccp **12**, 5503 (2010).

[8] J. J. Rehr, J. J. Kas, M. P. Prange, A. P. Sorini, Y. Takimoto, and F. Vila, Comptes Rendus Physique **10**, 548 (2009).

[9] R. S. Markiewicz, S. Sahrakorpi, and A. Bansil, Phys. Rev. B **76**, 174514 (2007).

[10] R.S. Markiewicz, Tanmoy Das, Susmita Basak, and A. Bansil, Journal of Electron Spectroscopy and Related Phenomena **181**, 23 (2010).

[11] G. Onida, L. Reining, and A. Rubio, Rev. Mod. Phys. **74**, 601 (2002).

[12] S. Basak, T. Das, H. Lin, J. Nieminen, M. Lindroos, R. S. Markiewicz, and A. Bansil, Phys. Rev. B **80**, 214520 (2009).

[13] S. Basak, T. Das, H. Lin, R. S. Markiewicz, and A.Bansil (2010), march meeting (APS), URL `http://meetings.aps.org/link/BAPS.2010.MAR.Q41.7`.

[14] N. Nücker, J. Fink, J. C. Fuggle, P. J. Durham, and W. M. Temmerman, Phys. Rev. B **37**, 5158 (1988).

[15] M. Klauda, J. Markl, C. Fink, P. Lunz, G. Saemann-Ischenko, F. Rau, K.-J. Range, R. Seemann, and R. L. Johnson, Phys. Rev. B **48**, 1217 (1993).

[16] H. Romberg, M. Alexander, N. Nücker, P. Adelmann, and J. Fink, Phys. Rev. B **42**, 8768 (1990).

[17] We use the term 'Mott gap' to denote the pseudogap in the CuO_2 plane.

[18] D. C. Peets, D. G. Hawthorn, K. M. Shen, Y.-J. Kim, D. S. Ellis, H. Zhang, S. Komiya, Y. Ando, G. A. Sawatzky, R. Liang, et al., Phys. Rev. Lett. **103**, 087402 (2009).

[19] J. J. Rehr and A. L. Ankudinov, Radiation Physics and Chemistry **70**, 453 (2004).

[20] J. A. Soininen, J. J. Rehr, and E. L. Shirley, Physica Scripta **T115**, 243 (2005).

[21] U. von Barth and L. Hedin, J. Phys. C **5**, 1629 (1972).

[22] A. L. Ankudinov and J. J. Rehr, Phys. Rev. B **62**, 2437 (2000).

[23] R. S. Markiewicz, S. Sahrakorpi, M. Lindroos, H. Lin, and A. Bansil, Phys. Rev. B **72**, 054519 (2005).

[24] Effects of doping are treated at the rigid-band level.[25]

[25] A. Bansil, Zeitschrift Naturforschung A **48**, 165 (1993).

[26] E. Pellegrin, N. Nücker, J. Fink, S. L. Molodtsov, A. Gutiérrez, E. Navas, O. Strebel, Z. Hu, M. Domke, G. Kaindl, et al., Phys. Rev. B **47**, 3354 (1993).

[27] N. Kosugi, Y. Tokura, H. Takagi, and S. Uchida, Phys. Rev. B **41**, 131 (1990).

[28] M. Braden, P. Schweiss, G. Heger, W. Reichardt, Z. Fisk, K. Gamayunov, I. Tanaka, and H. Kojima, Physica C: Superconductivity **223**, 396 (1994).

[29] It will be interesting to examine effects of La/Sr substitution on apical O sites beyond the rigid band model using first-principles approaches.[30]

[30] A. Bansil, S. Kaprzyk, P.E. Mijnarends, and J. Tobola, Phys. Rev. B **60**, 13396 (1999); S. Kaprzyk and A. Bansil, Phys. Rev. B**42**, 7358 (1990).

[31] C. T. Chen, F. Sette, Y. Ma, M. S. Hybertsen, E. B. Stechel, W. M. C. Foulkes, M. Schulter, S.-W. Cheong, A. S. Cooper, L. W. Rupp, et al., Phys. Rev. Lett. **66**, 104 (1991).

[32] A. Liebsch, Phys. Rev. B **81**, 235133 (2010).

[33] X. Wang, L. de' Medici, and A. J. Millis, Phys. Rev. B **81**, 094522 (2010).

[34] H. Eskes, M. B. J. Meinders, and G. A. Sawatzky, Phys. Rev. Lett. **67**, 1035 (1991).

[35] M. C. A. Comanac, L de Medici and A. J. Millis, Nature Physics **4**, 287 (2008).